

1 Problems of Global Ocean Averages and Integrals
2 Not peer reviewed. Submitted to Tellus for publication.

3 Carl Wunsch
 Department of Earth and Planetary Sciences, Harvard University
 Cambridge MA 02138 USA
 Department of Earth, Atmospheric and Planetary Sciences
 MIT, Cambridge MA 02139 USA
 email: carl.wunsch@gmail.com
 Orcid No. 0000-0001-6808-3664

4 July 10, 2026

5 **Abstract**

6 The ocean circulation exhibits a great regional variation in the temporal behavior of phys-
7 ical parameters such as temperature or salt or carbon. Some of the variety is very familiar,
8 e.g. equatorial versus mid-latitude, but in addition much heterogeneity appears within those
9 very large-scale geographical regions. Questions arise in computing and understanding the
10 meaning of such quantities as the global average temperature or heat uptake and their cor-
11 responding uncertainties. Heat content through space and time in the abyssal ocean, below
12 2000m, as seen in a 26-year state estimate, is used as an example.

13 **1 Introduction**

14 For many purposes, both descriptive and analytic, a knowledge of characteristics of quantities
15 applying globally to the Earth is useful. An example is the mean temperature of the global
16 ocean, acting both as a description relative e.g., to geological-past-states, and as an element of
17 energy components of the present climate system. This utility persists despite what is quite
18 clearly vast regional differences that require description and analysis in many geographical vari-
19 ations. Similar statements can be made about descriptive elements of global health and general
20 econometric variables, whose statistical problems overlap the oceanographic one.

21 The project called Estimating the Circulation and Climate of the Ocean (ECCO) has pro-
22 duced a 26 year-estimate (starting in 1992) of the global ocean circulation that combines a

23 numerical model of the circulation with most of the available global data sets. This particular
24 product, labelled version4 release 4 (ECCOv4r4), was constructed by procedures discussed by
25 Wunsch and Heimbach (2014), and Forget et al. (2015). The process can be summarized as one
26 treating the inverse problem of estimating the ocean circulation from the numerical representa-
27 tion of the appropriate equations of motion in quantitative combination with observations, all
28 subject to quantitative estimates of the errors inevitably present in both data and numerical
29 models.

30 Extended descriptions of the results can be found in Fukumori et al. (2018), ECCO Consor-
31 tium et al. (2021), Wunsch, 2024, hereafter W24; Wunsch, 2025, hereafter W25) and will not
32 be repeated here. For present purposes, the main properties are that the estimate, computed
33 with a nominal 1 hour time-step, 50-vertical layers, and a horizontal resolution of nominal order
34 1 deg of latitude and longitude although varying, satisfies a free-running version of the MITgcm
35 (Adcroft et al., 2004) and is generally consistent within error estimates of the observations as
36 described in ECCO Consortium et al. (2021). Because the model contains “controls” (including
37 initial and surface boundary conditions) which have been adjusted so that the consequent free-
38 running model is generally consistent with the data, one is assured that the physical conservation
39 laws (energy, mass, potential vorticity, etc.), vitally important to physical interpretation, are
40 satisfied up to the numerical accuracy of the GCM.¹

41 In W24,W25, the ECCOv4r4 estimate was time-averaged over the full 26-year period and
42 some of the elements of the average were displayed and described. For present purposes, a few of
43 the gross properties that emerged are of interest: (1) Over much of the ocean many of the physical
44 parameters (e.g., temperature, velocity) exhibit long period changes precluding the inference that
45 the time-mean represents a steady-state. (2) Along with that inference was the indication of
46 underlying temporal variability inconsistent with any assumption of a *statistically* steady state.
47 (3) Much regional structure in the physics of the time-mean is apparent. (4) Conventional
48 default assumptions of near-Gaussian statistics of the temporal and spatial variability are often
49 violated.

50 Taken together, these results suggest difficulties in the best computation of quantities such as
51 the global oceanic mean temperature and its trends. The ECCOv4r4 result remains an estimate
52 of the ocean circulation, and is not the circulation itself. The literature cited above discusses the
53 extent to which elements have been observed and the degree to which those data are reproduced

¹One might compare the ECCO estimate to the apparently similar meteorologically-originated “reanalyses.”
As discussed e.g., by Wunsch, Williamson, Heimbach (2023), those products are subject to a kind of uncertainty
principle, in which the sequential injection of observations changes the estimated state—in the process violating
the conservation laws.

54 within error estimates—themselves subject to uncertainties. For present purposes, it will only be
 55 assumed that the estimate reproduces much of the character of the real temporal fluctuations and
 56 their multi-decadal means, with the intention of exploring a few of the implications. Statisticians
 57 (e.g., Wilcox, 2010) emphasize that such problems do not have a “right” answer—merely ones
 58 that can be useful as descriptors or predictors or providers of insight.²

59 Description of the global ocean circulation and its variability is a challenging task. Here,
 60 intending only to be exemplary, the focus is put on the water column heat content below 2000m—
 61 a subject of intense interest in the wider climate science framework, and one that to some
 62 extent amplifies the problems. (See e.g., Hakuba et al., 2024, for a general review of the climate
 63 framework.)

64 Oceanic mean temperatures, and its divisions along with salinity defining oceanographic “wa-
 65 ter masses”, have long been a central descriptor of oceanic structure (e.g. Worthington, 1981).
 66 The ECCOv4r4 state estimate employs almost all of the extant temperature measurements in
 67 the interval following 1992 including those from the traditional global ship observations and the
 68 Argo data from many thousands of free drifting floats. It remains true however, that the great
 69 bulk of those latter data pertain to the upper 1-2km of the ocean with the abyssal estimates
 70 relying heavily upon the model physics plus such other data as the altimetry and meteorology.³

71 W25 has a more extended summary of some of the statistical issues and as applied to sea
 72 level, the total water column heat content, and the abyssal sub-element. The purpose of the
 73 present note is to elaborate, and partially correct, some of that discussion as it applies to the
 74 abyss.

75 2 The Ocean Below 2000m. Heat Content

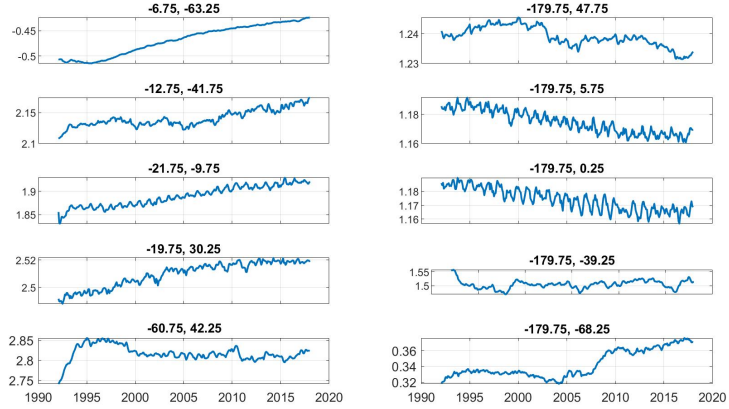
76 Let $\theta(\mathbf{r}, z, t)$ be oceanic potential temperature, where \mathbf{r} is the lateral position vector (latitude,
 77 longitude), z the vertical coordinate, and t is time. All variables are discrete. Heat content
 78 below 2000m is approximately,

$$Q_a(\mathbf{r}_i, t) = c_p \rho_0 \int_h^{-2000} \theta_a(\mathbf{r}_i, z, t) dz, \text{ J/m}^2 \quad (1) \quad \{\text{Qa1}\}$$

79 $c_p = 3994 \text{ J/kg/}^\circ\text{C}$ an approximate heat capacity, $\rho_0 = 1038 \text{ kg/m}^3$ a reference density, and h is
 80 the local water depth, taken as negative. (The Q_a values computed here are based upon degrees

²The language used in much of the statistics literature, with its overlay of philosophy, is commonly very much stronger, sometimes startlingly so, than is commonly found in the wider scientific literature. See for example, Jaynes (2003).

³See Hennon et al. (2019) as one example of myriad data issues.



10.614700in19.999599in

Figure 1: (left panel) Example time series of the vertical abyssal average (2000m to the bottom) temperature $\bar{\theta}_a$, at 5 locations in the Atlantic Ocean. Units °C. South to north. Labels are longitude, latitude respectively. See Fig. 2 for positions. W25b displayed some of the total heat content time series. (Right panel) Same as left panel except for the Pacific Ocean along 180°W and showing some notable cooling. W25, Fig. 16, provides some comment on the appearance in some regions of an annual cycle in the abyss.

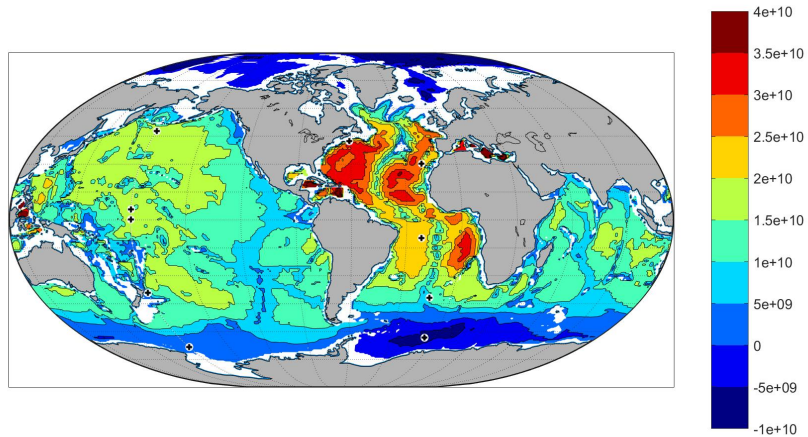
{temper_timese

81 Celsius, which permits negative values. Absolute temperatures, degrees Kelvin, required for en-
 82 ergy discussions, preclude the negative values displayed here in some areas. For a full discussion
 83 of the energetics of a water column see, for example, Vallis, 2017). A cogent argument can be
 84 made that the upper limit of the integral should be an isopycnal. That however, introduces
 85 another space-time variable that is not important for the present purposes Vertical average
 86 temperature is,

$$\bar{\theta}_a(\mathbf{r}_i, t) = \frac{Q_a(\mathbf{r}_i, t)}{c_p \rho_0} / (-2000 - h). \quad (2)$$

87 These values were computed at grid points spaced at 1° of longitude and 1/2° of latitude.
 88 Some coincide with the model grid and some are interpolated values. Fig. 1 displays a few of the
 89 time series of vertically averaged potential temperatures at fixed positions in the Atlantic and
 90 Pacific Oceans. The visual melange, which is not exhaustive, is an indication of the numerous
 91 ways in which the temporal variability influences any time average. Positions are shown in Fig.
 92 2. This spatial and temporal inhomogeneity raises questions of the physical interpretation of
 93 global averages in space and/or time.

94 An overbar will be used to denote vertical averages, and a bracket, $\langle \cdot \rangle$, for temporal ones.
 95 In some cases, the operation will refer to a median rather than a mean. Thus $\langle Q_a(\mathbf{r}, t) \rangle$ is a
 96 function of position, \mathbf{r} , alone. Note that areas corresponding to the grid points here are a strong
 97 function of latitude, vanishing at the north pole, and values of means/medians and trends on
 98 the grid must be distinguished from those that are appropriately area-weighted.



7.114800in13.333700in

Figure 2: Median in time of Q_a at each grid point (J/m^2). A map of the time average is visually indistinguishable from this one. + marks the positions of the time series in Fig. 1. Strong topographic control of heat content is apparent.

{qa_median_gri

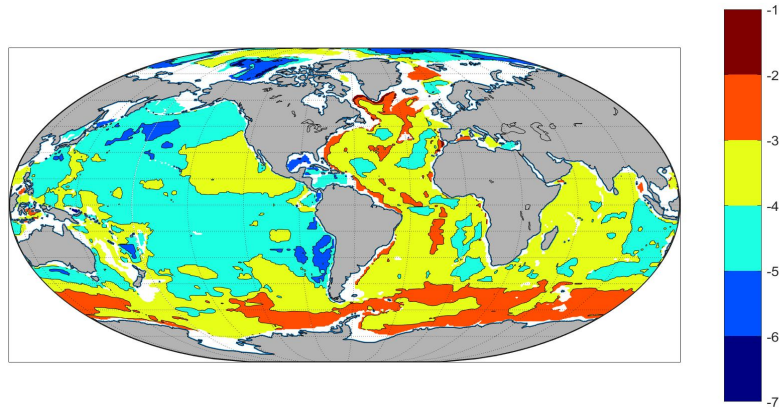
99 Default discussions of stochastic processes in an oceanographic context, but also in the wider
 100 geophysical/climate literature, almost inevitably assume near-Gaussian, statistically stationary
 101 processes. The statistics literature (e.g., Efron and Tibshirani, 1993) forcefully emphasizes that
 102 such assumptions can lead to seriously incorrect estimates from samples, particularly of the
 103 accuracy of values, should deviations, even sometimes slight, occur.

104 2.1 A Statistical Framework

105 A major issue in capturing the flavor of the great variations in the behavior of time (or space)
 106 series, such as shown in Fig. 1, is the extent to which the processes can be regarded as statistically
 107 stationary. That character is commonly assumed by default e.g., in computing confidence limits
 108 on such quantities as time-means and spectral estimates. As emphasized e.g., by Beran (1994),
 109 deviations from stationarity⁴ generally produce radically different statistical interpretations. To
 110 deal with the potential lack of stationarity, and the varying extent to which it can be violated,
 111 the statistical literature commonly relies upon a generalization of the mathematical machinery
 112 of autoregressive moving average (ARMA) representations used for fully stationary processes;
 113 see Chatfield (2004) or Box et al. (2008); or the summary in W25b). Mudelsee (2010) is a
 114 textbook treating some of the general peculiarities of climate space-time statistics.

115 The important characteristic of stationarity can fail e.g., if a linear trend is present. Defining

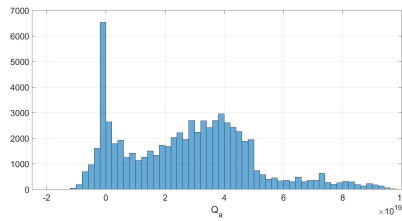
⁴We distinguish “stationary” here from its sometimes common use as implying steady flows.



9.947900in19.999599in

Figure 3: \log_{10} of the conventional variance of vertical average abyssal temperature (degrees C). High Southern and North Atlantic Ocean values appear, as does a comparatively quiet Western and South Pacific Ocean.

{var_thetaa_lo



9.947900in19.999599in

Figure 4: Histogram of the time median values Q_a weighted by area at each grid point (Joules). The time-mean values are nearly identical. Non-normal (non-Gaussian) behavior appears. Here and elsewhere a very small number of outlying values are omitted.

{histograms_qa

116 the backwards difference operator $B\xi_t = \xi_{t-1}$, a stationary process in that situation can then
 117 be generated by taking the difference,

$$w_i = \xi_i - \xi_{i-1} = (1 - B) \xi_i$$

118 an ARMA(p, q) representation including ξ_t is then possible,

$$\sum_{i=1}^p \phi_i w_i = \sum_{i=1}^q \psi_i \varepsilon_i \quad (3) \quad \{\text{A1}\}$$

119 where ε_i is commonly a white noise process and the constants ϕ_i and ψ_i are the coefficients
 120 of the autoregressive and moving average representations respectively. The result is generally
 121 labelled an autoregressive integrated moving average (ARIMA($p, 1, q$)). The desirable properties
 122 of the polynomials generated from ϕ_i, ψ_i are discussed in the references, as are the best choices
 123 choices of p, q from various statistical tests. Solving Eq. (3) for w_i ,

$$w_i = \left(\sum_{i=1}^p \phi_i B^i \right)^{-1} \sum_{i=1}^q \psi_i \varepsilon_i, \quad (4)$$

124 existence of the polynomial inverse being guaranteed by the requirements on its determination.

125 A simple backwards difference is too restrictive for present purposes. The system is general-
 126 ized by defining,

$$\xi_i = (1 - B)^d w_i, \quad (5) \quad \{\text{A2}\}$$

127 where d need not be an integer and,

$$(1 - B)^d = \sum_{j=0}^{\infty} (-1)^j \frac{\Gamma(d+1) B^j}{\Gamma(j+1) \Gamma(d-j+1)} \quad (6) \quad \{\text{one_minus_B}\}$$

128 where Γ is the gamma function (Beran et al., 2013, P.47) . The original, non-stationary, w_i , is,

$$w_i = (1 - B)^{-d} \left(\sum_{i=1}^p \phi_i B^i \right)^{-1} \sum_{i=1}^q \psi_i \varepsilon_i. \quad (7)$$

129 Behavior of the series varies greatly with d , ranging from stationary ($d \leq 0$), to explosively
 130 growing for large values, $d > 1$. The general formulation with arbitrary d in Eq. (3) is labelled
 131 an ARIMA(p, d, q). Here d will be used as a descriptor of oceanic variability.

132 Note that in some contexts, the Hurst parameter, originating in hydrology, $H = d + 1/2$,
 133 is more familiar. Table 1, from W25 and Brockwell and Davis (1991), provides a listing of the
 134 behavior of time series as a function of the values of d, H . As in W25, a distinction is made
 135 between “long autocovariance memory” and “long physical memory,” where in the terminology

d	$H = d + 1/2$	Character
$0 < d \leq 1/2$	$1/2 < H \leq 1$	Stationary, long autocovariance memory
0	1/2	Stationary white noise
$-1/2 < d \leq 0$	$0 < H \leq 1/2$	Stationary, short autocovariance memory
$d \leq -1/2$	$H < 0$	Stationary
$d > 1/2$	$H > 1$	Non-stationary, long physical memory

Table 1: General behavior of a time series for a given value of d . H is the corresponding Hurst parameter used particularly in the hydrological literature. From W25. Stationarity implies a local statistical equilibrium not dependent upon earlier initial conditions, while non-stationarity likely means that dependence is still present in the ocean. Discussion can be found in Brockwell and Davis (1991), Beran (1994), Chatfield (2004), Box et al. (2008) and elsewhere. Long autocovariance memory refers to processes whose autocovariances decay much more slowly than those for conventional processes and are distinguished here from long physical memory processes.

136 of Beran (1994), long autocovariance memory refers to the slow decay of the autocovariance
137 relative to that expected for a stationary normal process, and is distinguished here from long
138 physical memory involving oceanic processes having time-scales longer than the duration of
139 observations—extending to thousands of years.

140 Among numerous other properties, as described in W25, d determines the estimated variance
141 of e.g., an estimated sample mean. Thus for $d = 1/2$, (a random walk) the uncertainty of a
142 sample mean does *not* diminish with increasing numbers of samples, M . For larger values of d ,
143 variance *increases* with M . $d = 0$ produces the familiar conventional behavior of the variance
144 of a Gaussian process sample mean decreasing with M .

145 Determination of d can be made by different methods. The one with the most immediate
146 physical interpretation derives it from the estimated power spectrum of the process,

$$\Phi(s) \approx s^{-2d}, \quad s \rightarrow 0, \quad (8)$$

147 where s is the frequency or equivalent. Values of d become descriptors of the familiar spectral
148 behavior of “blue noise” ($d < 0$), “white noise” ($d = 0$), “red noise” ($d > 0$), “non-stationary
149 rednoise” ($d > 1/2$) etc. (see Table 1). The general subject of spectral behavior of climate
150 variables, not discussed here, has been the focus of considerable effort. von Storch et al. (2001)
151 describe many of the general properties.

152 Here, estimated values, \tilde{d} , are determined from a least-squares fit to the 10 lowest frequencies
153 in the periodograms of monthly-varying temperature (periods longer than the annual). Hurvich
154 and Ray (1995) discuss the sometimes complicated biases in this calculation, called by them the

155 GPH test, and which can be a strong function of d . If the periodograms have been computed
 156 using a bell taper, they suggest omitting the periodogram estimate at the lowest non-zero fre-
 157 quency. In the present case, no taper has been used, and no bias correction has been attempted.
 158 As with many results recorded here, estimates of d should be regarded as tentative, with a
 159 primarily qualitative connotation.

160 2.2 Spatial Means/Medians

161 By integrating over the entire global ocean, one has the complete population, and not a sample,
 162 and which renders moot much of the conventional statistics discussion (see for example, Rice,
 163 2007, Ch. 7) applicable to finite limited samples. In the abstract, one might regard the existing
 164 oceanic state as simply one member taken from an ensemble of hypothetical Earths each subject
 165 to statistically varying climate systems. That assumption, for example, can justify the use, as
 166 in W25, of a bootstrap for discussing statistics. In the present case, that possibility is set aside
 167 as it ultimately demands a statement of the statistics governing the ensemble. The approach
 168 assumed that all values come from an independent identically distributed (iid) collection (Efron
 169 and Tibshirani, 1993), and which in practice cannot be justified for subsamples of $\langle Q_A(\mathbf{r}_i) \rangle$.

170 (1) *The Mean and Median*

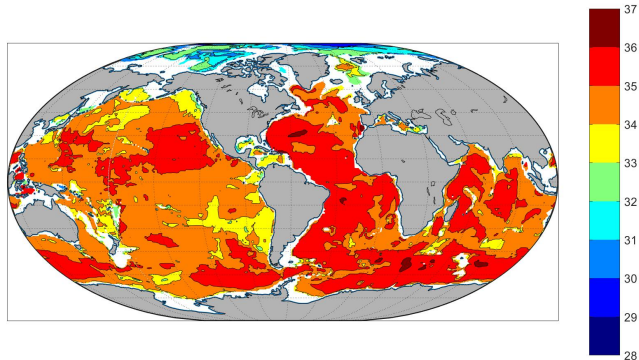
171 Let ΔA_i be the area represented by the grid point at \mathbf{r}_i . Total area is $A = \sum_1^N \Delta A_i$. Then
 172 the mean value is simply,

$$m_1 = \frac{1}{A} \sum_{i=1}^N \langle Q_A(\mathbf{r}_i) \rangle \Delta A_i \quad (9)$$

173 producing, $m_1 = 1.26 \times 10^{10} \text{ J/m}^2$, the 26-year average value.

174 A median value (median $(Q_A(\mathbf{r}_i, t) \Delta A_i / \text{median}(\Delta A_i))$) is nearly indistinguishable at $1.16 \times$
 175 10^{10} J/m^2 and see Fig. 2. Estimating the accuracy of such values will depend upon any
 176 systematic and stochastic errors both in the underlying model representations and in the multiple
 177 data sets used there, and is not attempted. (A covariance of an estimated uncertainty is a square
 178 matrix of dimension of the state vector, which in this case exceeds 10^7 values at any one time.)
 179 Whether the small difference between the mean and median here is of any importance can only
 180 be decided in the context of their use.

181 Fig. 5 displays the logarithm of the area weighted temporal variance in $\langle Q_a(\mathbf{r}_i, t) \Delta A_i \rangle$. The
 182 very small values in the Arctic Sea are prominent, arising primarily from the very small grid
 183 spacing near the pole, but also from the small temporal range of estimated temperatures there.
 184 An inference that variance-weighted forms of these values should dominate the global average



7.114800in13.333700in

Figure 5: \log_{10} of the area weighted variance of the temporal variability in Q_a (joules). The very low values in the high Arctic Sea are notable. These would give a high weight to $\langle Q_a \rangle$ in a variance weighted spatial mean—not discussed here.

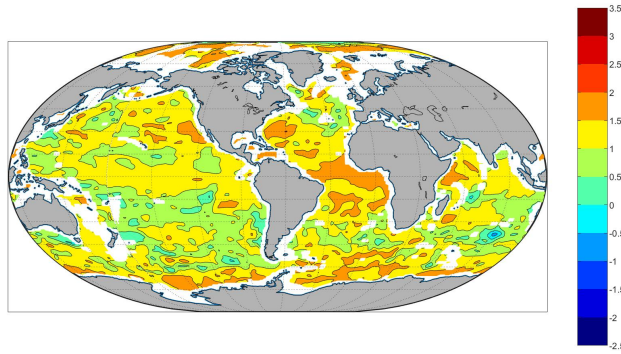
{rqa_map.jpg}

185 (it is negative with a very small uncertainty) is rejected on physical grounds. Furthermore, any
 186 assumption of spatially uncorrelated fields cannot be defended.

187 (2) *Means/medians stratified by d*

188 An estimate of d was made in W25 from the low-frequency least-squares fit slopes of the
 189 logarithms of the power spectra/periodograms at each grid point and a spatially smoothed esti-
 190 mate is shown here in Fig. 6. Because \tilde{d} is itself an estimate, it has a corresponding uncertainty
 191 measured by the residual in the periodogram fits. Fig. 7 is the unsmoothed result except that
 192 regions where \tilde{d} is indistinguishable from 0—ordinary stationarity—are shown as blank areas.
 193 Much of the visual complexity, as with the ordinary temporal variances, is undoubtedly due to
 194 the complexity of the model bottom-topography, subject to the caveat that it remains greatly
 195 under-resolved.

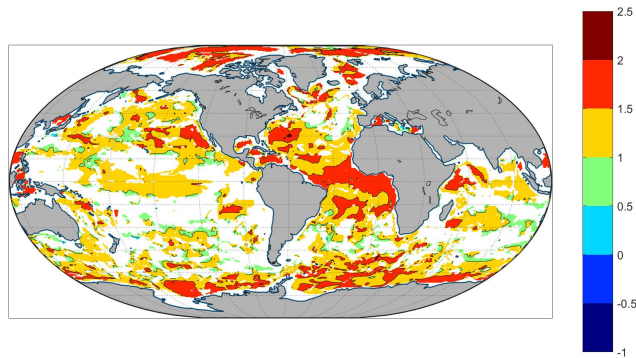
196 “Stratified” means and medians (e.g., see Kendall and Stuart, 1973 or Rice, 2007) are com-
 197 puted for the different ranges of \tilde{d} , noting that these regions are generally not geographically
 198 contiguous and the samples are complete—that is they are not a random sample. Using ordi-
 199 nary sampling statistics in what is a homogeneous environment—at least as defined by \tilde{d} —the
 200 result is shown in Table 2. Despite the full population, twice the ordinary standard deviations
 201 of the means are listed for each region as a measure of noisiness. If interpreted as a random
 202 sample, neither of the largest areas produces a mean or median differing statistically from zero.
 203 The corresponding areas show that the bulk of the abyssal variability has long autocovariance
 204 memory or more general non-stationarity. Time averages in such a situation are not easy to
 205 interpret. In particular, the system must be regarded, despite the multi-decadal averaging, as



6.562200in8.750200in

Figure 6: \tilde{d} for the $ARIMA(p, d, q)$ determined by least-squares from the periodograms at each point and smoothed over 4 degrees of longitude and 2 degrees of latitude. (Unsmoothed version is in W25, Fig. 14.)

{dqasmth.jpg}



7.114800in13.333700in

Figure 7: Unsmoothed version of Fig. 6 except regions not differing at two standard deviations from $\tilde{d} = 0$, an ordinary stationary time series are left as blank and that value assigned everywhere there. Values of $\tilde{d} < 0$ are nearly non-existent; see Table 2. (Bottom topography remains a simplified version of the fully resolved field.)

{dqasig_ls.jpg}

\tilde{d}	mean/ 10^{10} J	median/ 10^{10} J	No. Vals.	Area/ 10^{13} m ²
$d \leq -1/2$	1.00±0.40	1.09	27	0.0065
$-1/2 \leq \tilde{d} < 0$	0.97±0.88	0.98	324	0.078
$0 \leq \tilde{d} < 1/2$	1.11±1.66	1.01	3689	0.765
$1/2 \leq \tilde{d} < 1$	1.19±1.32	1.13	18619	4.439
$1 \leq \tilde{d} < 2$	1.30±2.38	1.20	45547	9.655
$2 \leq d$	1.43±4.09	0.27	88	0.0142

Table 2: Values of the mean and median of Q_a in the different ranges of d . Mean and median differ significantly only for the small population $d_i=2$. Uncertainty values are 2 standard deviations of the means. Uncertainty of the median can be computed from a bootstrap, but is omitted here. Modified from W25.

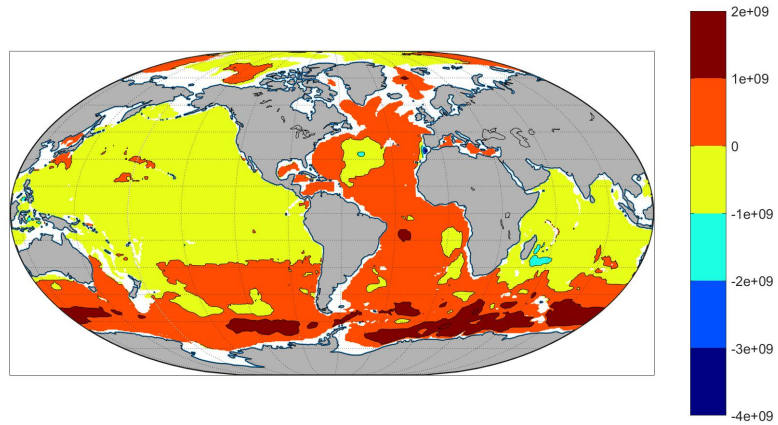
206 being far from anything resembling a steady-state.

207 Taken altogether, and coupled with the charts of values, the simplest inference here is that
 208 the heat content of the abyss, *measured in degrees Celsius*, is indistinguishable from zero. Further
 209 stratification by combined d and basin geography is obviously possible. Because of the variable
 210 area weighting and number of points, the global mean, \tilde{m}_1 , is not simply related to the means
 211 of Table 2.

212 3 Global Trends

213 Of more immediate interest in the climate change context is the extent to which the abyssal ocean
 214 has been a sink of heat from a warming atmosphere. Consider first Fig. 8. Medians of $Q_a(\mathbf{r},t)$ on
 215 each grid point for year 26 and for year 1 were subtracted and divided by 26 years. A generally
 216 large-scale pattern in the rates is evident, including the major regions of cooling. A value of
 217 10^7 J/m²y corresponds to 0.32W/m². The figure demonstrates a fundamental difficulty—that
 218 whatever global mean or median is found, it will be a small residual of large numbers. That
 219 large regions in the Southern and Atlantic Oceans have been undergoing strong warming is
 220 evident and uncontroversial. Cooling in the abyssal Pacific Ocean has been discussed e.g., by
 221 Bindoff and Mcdougall (1994), Meza and Gebbie (2025), and the Southern Ocean warming by
 222 Johnson and Purkey (2024) and others.

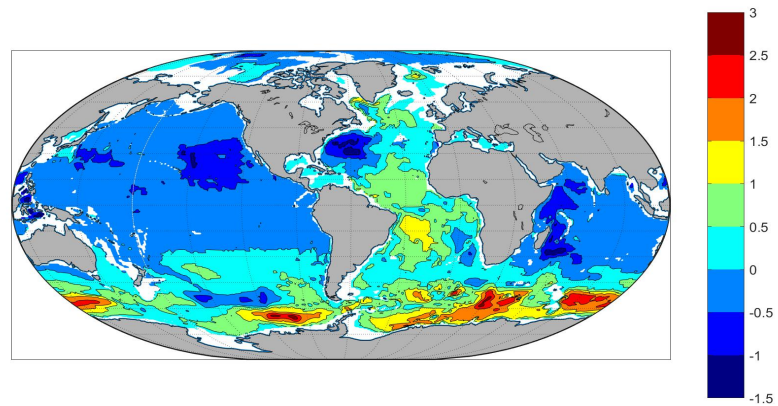
223 One criticism of the simple difference approach is that determining a trend by taking the
 224 difference of two averaged years ignores the information contained in the 312 monthly values
 225 occurring between the start and finish of the state estimate. To address that shortcoming, resort
 226 is now had to the so-called Theil-Sen (ThS) median, following the discussion in Wilcox (2010).



7.114800in13.333700in

Figure 8: Rate of change of Q_a J/m²y from the difference of the time median values over the last and first years. Large regions of both positive and negative values appear. 10^7 J/m²y=0.32W/m²

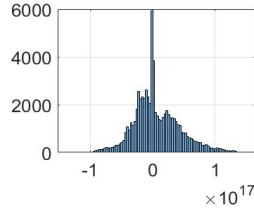
{qalastyr_minu



9.947900in19.999599in

Figure 9: Grid point values, converted to W/m² of the Theil-Sen median trend in Q_a . Gross patterns are similar to those of Fig. 8 but much difference in detail appears.

{qatimetrend_t



4.375100in5.833200in

Figure 10: Area weighted Theil-Sen median values of the time trend, Joules/y, at each grid point. Non-normality is again apparent.

{histogram_qat

227 The ordinary median estimator, itself more robust than least-squares is, for a sequence ξ_j ,
 228 the middle value of successive pairs, $\xi_j - \xi_{j-1}$. In contrast, the Theil-Sen estimator computes
 229 the median of *all* pairs $(\xi_j - \xi_{j'}) / (j - j')$, $j \neq j'$, which in a sequence of M values produces
 230 $M(M - 1)/2$ pairs for estimation in each sequence.

231 Applying the Theil-Sen algorithm as encoded in Matlab (Tilgencamp, 2025) to each grid
 232 point results in the trend/year estimates shown in Fig. 9, but converted to W/m^2 . Although
 233 there exists a strong resemblance to Fig. 8, many detailed pattern differences appear. The
 234 ordinary spatial average of the area weighted estimate of $\Delta Q_{ai} \Delta A_i / \Delta t = 2.79 \times 10^6 \text{J}/\text{m}^2/\text{y}$. If
 235 an ordinary least-squares fit is used to determine the temporal trend instead of the ThS estimate,
 236 the values are indistinguishable within the uncertainty estimate of Gaussian least-squares. In
 237 a spatial map of the difference of the mean and median values of $\Delta Q_{ai} \Delta A_i / \Delta t$, the region of
 238 largest difference is in the western North Atlantic Ocean just east of the Gulf Stream.

239 *Stratified values*

240 Values when stratified by \tilde{d} as above, produce the results shown in Table 3. As with the
 241 time means, the values apply primarily to non-statistically stationary regions, or those with long
 242 autocovariance memory. In a regional discussion, not offered here, this different behavior would
 243 have to be accommodated.

244 4 Discussion

245 As already noted above, the statistics literature reminds one that definitive answers to statistical
 246 problems rarely exist—procedures must be analyzed and interpreted within the physical context
 247 of any particular problem. Determining the global ocean average of any quantity, whether it be
 248 via a state estimate, or a particular instrument set, faces the special problems of a continuum
 249 with highly heterogeneous statistical properties. Not discussed here is the issue of how much

\tilde{d}	mean ThS/ $10^6\text{J}/\text{m}^2\text{y}$	median ThS/ $10^6\text{J}/\text{m}^2\text{y}$	No. Vals.	Area/ 10^{13}m^2
$d \leq -1/2$	1.16 ± 0.0019	1.36	27	0.0065
$-1/2 \leq \tilde{d} < 0$	0.36 ± 4.29	-0.015	324	0.078
$0 \leq \tilde{d} < 1/2$	-0.18 ± 12.7	-0.016	3689	0.765
$1/2 \leq \tilde{d} < 1$	0.36 ± 2.16	-1.14	18619	4.439
$1 \leq \tilde{d} < 2$	4.16 ± 39.59	0.50	45547	9.655
$2 \leq d$	6.7 ± 7.29	2.39	88	0.0142

Table 3: Values of the mean and median of the Theil-Sen (ThS) time trend in the different ranges of d . Except for the minute area of $d_j = -1/2$, none of the median or mean values is significant at 2 standard deviations. $10^6 J/my = 0.03W/m$

250 of these changing fields should be regarded as deterministic e.g., by a warming atmosphere,
251 and how much stochastic. Calculation of global mean or median values is straightforward, but
252 determining their accuracy and the significance of any apparent change with time or space is
253 subject to a long list of assumptions—combining the purely physical with the purely statistical.
254 As the result of a state estimate of a state vector of very large dimension, present values cannot
255 be readily evaluated in absolute accuracy terms. These problems are generic.

256 In a fundamental way, description of the ocean circulation appears to require methods ir-
257 retrievably regional in nature. The great heterogeneity in the underlying variability precludes
258 regarding even a near-three-decade averaging interval as representing a system close to a steady-
259 state overall. But the physics of regional values and changes nonetheless do depend upon the
260 global values and changes.

261 The state estimate has much less noise than does any particular near-global observational
262 data set—lacking explicit internal waves, mesoscale (balanced), and sub-mesoscale eddies, as well
263 as a simplified set of boundary conditions. As such, much of the expected error is systematic—
264 lying in the various parameterizations of internal waves, and of interior and boundary turbulence.
265 Systematic errors should have a greater influence on e.g., the time means/medians than on
266 temporal differences—whether explicit year differences, or through the determination of trends
267 by successive differencing of the (here) monthly values. Spatial differences entail many different
268 potential systematic problems. Full understanding of systematic errors involves evaluation of
269 the impacts of the various parameterizations, the limited resolution of the model representation,
270 and calibration problems of the underlying observational data.

271 Whether a mean or median is a more meaningful measure of the physical parameter is
272 often not very clear when the values differ significantly. The common use of time- or space-
273 averaged equations of motion tends to dictate use of the mean. But given situations in which

274 the distributions of properties are qualitatively non-normal, use of median value equations ought
275 at least to be considered. In the present state estimate, one not producing extreme numerous
276 outliers, means and medians are nearly interchangeable. Underlying the results is the measure
277 used within the state estimate of least-squares fits to time dependent data sets—data sets which
278 themselves may have highly non-normal distributions with outliers. That likely dictates ultimate
279 use of more robust measures of misfit.

280 With its primary focus on the spatial heterogeneity, this paper refrains from examining
281 existing published estimates of mean ocean abyssal heat content and which evidently demands
282 a region-by-region approach. That strong warming has taken place over much of the Southern
283 and Atlantic Oceans is not in dispute, but the meaning of the global averages remains unclear.
284 Such diverse fields as human health care and econometrics share many of the issues raised here,
285 but no sufficiently general statistical tools appear to exist accommodating all of the complexity
286 found.

287 *Acknowledgments.* Self-funded. All values used here are the result of the ECCO Project
288 efforts, and all are available via the NASA websites. No ethics clearance required.

289 **References**

- 290 Adcroft, A., J. M. Campin, C. Hill and J. Marshall (2004). Implementation of an atmosphere-
291 ocean general circulation model on the expanded spherical cube. *Monthly Weather Review* 132(12):
292 2845-2863.
- 293 Anderson, D. L. T., K. Bryan, A. E. Gill and R. C. Pacanowski (1979). Transient-response of the
294 North Atlantic-some model studies. *Journal of Geophysical Research-Oceans and Atmospheres*
295 84(NC8): 4795-4815.
- 296 Beran, J. (1994). *Statistics for Long Memory Processes*. Chapman and Hall, New York.
- 297 Bindoff, N. L. and T. J. McDougall (1994). Diagnosing climate change and ocean ventilation
298 using hydrographic data. *J. Phys. Oc.* 24(6): 1137-1152.
- 299 Box, G. E. P., G. M. Jenkins and G. C. Reinsel (2008). *Time Series Analysis: Forecasting and*
300 *Control*. Hoboken, N.J., John Wiley.
- 301 Brockwell, P. J. and R. A. Davis (1991). *Time Series: Theory and Methods* 2nd Ed. New York,
302 Springer-Verlag.
- 303 Chatfield, C. (2004). *The Analysis of Time Series. An Introduction*, Sixth Ed. Boca Raton,
304 Chapman and Hall/CRC.
- 305 ECCO Consortium, I. F., O. Wang, I. Fenty¹, G. Forget, P. Heimbach, R. M. Ponte (2021)
306 Synopsis of the ECCO Central Production Global Ocean and Sea-Ice State Estimate, Version 4
307 Release 4. <https://zenodo.org/records/4533349>
- 308 Efron, B. and R. Tibshirani (1993). *An Introduction to the Bootstrap*. New York, Chapman
309 & Hall.
- 310 Forget, G., J.-M. Campin, P. Heimbach, C. Hill, R. Ponte and C. Wunsch (2015). ECCO version
311 4: an integrated framework for non-linear inverse modeling and global ocean state estimation.
312 *Geosci. Model Dev.* 8: 3071-3104.
- 313 Fukumori, I., P. Heimbach, R. M. Ponte and C. Wunsch (2018). A dynamically-consistent ocean
314 climatology and its temporal variations. *Bull. Am. Met. Soc.*, Oct.: 2107-2127.
- 315 Hakuba, M. Z., Fourest, S., Boyer, T. et al. (2024). Trends and variability in Earth's energy
316 imbalance and ocean heat uptake since 2005. *Surv. Geophys.* 45: 1721-1756.
- 317 Hennon, T. D., M. H. Alford and Z. X. Zhao (2019). Global assessment of semidiurnal internal
318 tide aliasing in Argo profiles. *J. Phys. Oc.* 49(10): 2523-2533.
- 319 Hurvich, C. M. and B. K. Ray (1995). Estimation of the memory parameter for nonstationary
320 or noninvertible fractionally integrated processes. *J. Time Series Anal.* 16(1): 17-41.
- 321 Johnson, G. C. and S. G. Purkey (2024). Refined estimates of global ocean deep and abyssal
322 decadal warming trends. *Geophys. Res. Lett.* 51, c2024GL111229: <https://doi.org/10.1029/2024GL111229>.

323 Kendall, M. G. and A. Stuart (1973). The Advanced Theory of Statistics, 3rd ed, Griffin, Lon-
324 don.

325 Mudelsee, M. (2014). Climate Time Series Analysis: Classical Statistical and Bootstrap Meth-
326 ods, Springer.

327 Rice, J. A. (2007). Mathematical Statistics and Data Analysis, 3rd Ed. Belmont, CA, Thomson.

328 Vallis, G. K. (2017). Atmospheric and Oceanic Fluid Dynamics: Fundamentals and Large-Scale
329 Circulation. Cambridge UK, Cambridge Un. Press.

330 Wilcox, R. R. (2010). Fundamentals of Modern Statistical Methods. Substantially Improving
331 Power and Accuracy, 2nd Ed. New York, Springer.

332 Worthington, L. V. (1981). The water masses of the world ocean: some results of a fine-scale cen-
333 sus. in, Evolution of Physical Oceanography. Scientific Surveys in Honor of Henry Stommel. B.
334 A. Warren and C. Wunsch, The MIT Press, Cambridge (<http://ocw.mit.edu/ans7870/textbooks/Wunsch/wunschto>
335 42-69.

336 Wunsch, C. (2024). A time-average ocean: Thermal wind and flow spirals. Prog. oceanog. 221.

337 Wunsch, C. (2025). Statistical features of an ECCO time-averaged state estimate: Sea level and
338 abyssal heat content. J. Phys. Oc. 55: 1859-1879.

339 Wunsch, C. and P. Heimbach (2014). Bidecadal thermal changes in the abyssal ocean and the
340 observational challenge. J. Phys. Oc. 44: 2013-2030.

341 Wunsch, C., S. Williamson and P. Heimbach (2023). Potential artifacts in conservation laws
342 and invariants inferred from sequential state estimation. Ocean Sci. 19: 1253-1275.